

A Direct-Indirect Hybridization Approach to Control-Limited DDP

Carlos Mastalli Wolfgang Merkt Josep Marti-Saumell
Joan Solà Nicolas Mansard Sethu Vijayakumar

Abstract—Optimal control is a widely used tool for synthesizing motions and controls for user-defined tasks under physical constraints. A common approach is to formulate it using direct multiple-shooting and then to use off-the-shelf nonlinear programming solvers that can easily handle arbitrary constraints on the controls and states. However, these methods are not fast enough for many robotics applications such as real-time humanoid motor control. Exploiting the sparse structure of optimal control problem, such as in Differential Dynamic Programming (DDP), has proven to significantly boost the computational efficiency, and recent works have been focused on handling arbitrary constraints. Despite that, DDP has been associated with poor numerical convergence, particularly when considering long time horizons. One of the main reasons is due to system instabilities and poor warm-starting (only controls). This paper presents *control-limited Feasibility-driven DDP* (Box-FDDP), a solver that incorporates a direct-indirect hybridization of the control-limited DDP algorithm. Concretely, the forward and backward passes handle feasibility and control limits. We showcase the impact and importance of our method on a set of challenging optimal control problems against the Box-DDP and squashing-function approach.

Index Terms—optimal control, differential dynamic programming, direct and indirect methods

I. INTRODUCTION

A. Motivation

OPTIMAL control is a powerful tool to synthesize motions and controls through task goals (cost / optimality) and constraints (e.g., system dynamics, interaction constraints, etc.). We can formulate it through *direct methods* [1], which first discretize over both state and controls as optimization variables, and then use general-purpose Nonlinear Programming (NLP) solvers such as SNOPT [2], KNITRO [3], and

This research was supported by (1) the European Commission under the Horizon 2020 project Memory of Motion (MEMMO, project ID: 780684), (2) the Engineering and Physical Sciences Research Council (EPSRC) UK RAI Hub for Offshore Robotics for Certification of Assets (ORCA, grant reference EP/R026173/1), and (3) the Alan Turing Institute. (Corresponding author: Carlos Mastalli.)

Carlos Mastalli and Sethu Vijayakumar are with the School of Informatics, University of Edinburgh, South Bridge EH8 9YL, U.K. and the Alan Turing Institute (e-mail: carlos.mastalli@ed.ac.uk; sethu.vijayakumar@ed.ac.uk).

Wolfgang Merkt is with the Oxford Robotics Institute, Department of Engineering Science, University of Oxford, Oxford OX1 2JD, U.K. (e-mail: wolfgang@robots.ox.ac.uk)

Josep Marti-Saumell and Joan Solà are with the Institut de Robòtica i Informàtica Industrial, Universitat Politècnica de Catalunya, Barcelona, Spain (e-mail: jmarti@iri.upc.edu; jsola@iri.upc.edu).

Nicolas Mansard is with the Gepetto Team, LAAS-CNRS, Toulouse 31400, France (e-mail: nicolas.mansard@laas.fr).

The manuscript contains comparisons of our novel optimal control approach against state of the art methods. Contact carlos.mastalli@ed.ac.uk for further questions about this work.

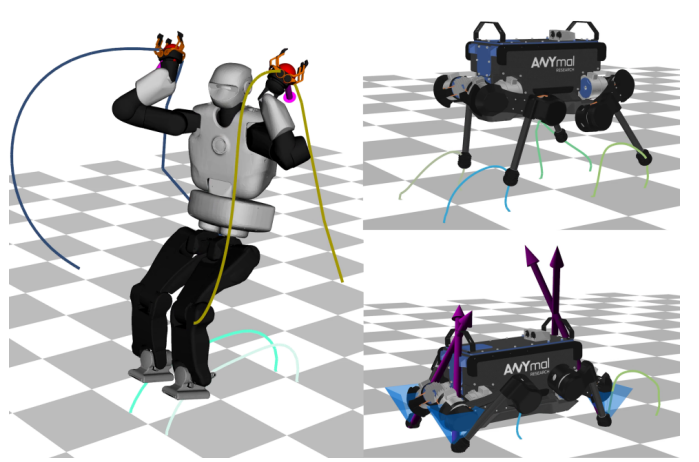


Fig. 1. Box-FDDP: a solver that incorporates a direct-indirect hybridization of the control-limited DDP algorithm. Challenging maneuvers computed by Box-FDDP: monkey bar and jumping tasks. The lines describe the trajectory performed by the hands and the feet.

IPOPT [4]. However, the main disadvantage of this approach is that it requires very large matrix factorizations, which limits its application domain to control on reduced models (e.g. [5], [6], [7]) or motion planning (e.g. [8], [9], [10], [11]).

Recent results on fast nonlinear Model Predictive Control (nMPC) based on DDP (e.g. [12], [13], [14], [15]) have once again attracted attention to *indirect methods*, which use the Pontryagin’s Maximum Principle (PMP) to first optimize the controls, and in particular, with its Gauss-Newton (GN) approximation called iterative Linear-Quadratic Regulator (iLQR) [16]. These methods impose and exploit a sparse structure of the problem by applying “Bellman’s principle of optimality” and successively solving the smaller sub-problems. This leads to fast and cheap computation due to very small matrix factorizations and effective data cache accesses. On the contrary, the main limitation compared with direct methods is the ability to efficiently encode hard constraints.

B. Related work

There are important recent achievements in both *direct-indirect* hybridization [17], [18] and handling input limits [19], as well as nonlinear constraints [20], [21], [22], [23], that are rooted in dynamic programming. For instance, Gifftthaler et al. [17] introduced a *lifted*¹ version of the Riccati equations that allows us to warm start both state and control trajectories.

¹This name is coined by [24], and we refer to *gaps* or *defects* produced between multiple shooting nodes.

In turn, Mastalli et al. [18] proposed a modification of the forward pass that numerically matches the gap contraction expected by a *direct multiple-shooting* method with only equality constraints. Unfortunately, both methods do not handle inequality constraints such as control limits. However, their hybrid approaches are numerically more robust to poor initialization because it is possible to warm start them with the state trajectory. Furthermore, with hybrid approach we refer to artificially include defect constraints (i.e. gaps on the dynamics) and the state trajectory as decision variables. These methods are hybrid since they attempt to solve optimal control necessary conditions by constructing the adjoint and the control equations, or any of the transversality (boundary) conditions, while still using the First-order Necessary Condition (FONC) of optimality for incorporating (artificially) the defect constraints.

There are two main strategies for incorporating arbitrary constraints: active-set and penalization methods (as extensively described in [25]). In the robotics community, one of the first successful attempts to incorporate inequality constraints in DDP used an active-set approach [19]. This early work focused on handling control limits during the computation of the backward pass, i.e. in the minimization of the control Hamiltonian². The method is popularly named Box-DDP, and the authors also showed a better convergence rate when compared with the squashing approach (i.e. a penalization method). Later, Xie et al. [22] included general inequality constraints into the control Hamiltonian and the forward pass. Despite that the method sacrifices the computational effort by including a second Quadratic Programming (QP) program in the forward pass, it still remains faster than solving the same problem using a direct collocation³ with SNOPT.

To overcome the main difficulties of traditional penalty function methods (i.e. ill-conditioning and slow convergence), Lantoine and Russell [27] proposed a method that incorporates an Augmented Lagrangian term. This method was studied in the context of robust thrust optimization, a much simpler case than the typical robotics problems. Later, Howell et al. [23] extended the Augmented Lagrangian approach to handle arbitrary inequality constraints for aerial navigation and manipulation problems. This latter work also used an active-set projection for solution polishing and showed to be often faster than direct collocation solved with IPOPT or SNOPT. Finally, a recent extension of the squashing approach [28] has shown competitive performance against the Box-DDP.

In this work, we bridge the gap between direct-indirect hybridization with control-limits inequalities. Other inequalities, e.g. on the state, can still be handled penalization as demonstrated in the results section.

C. Contribution

In this paper, we propose enhancements to the Box-DDP algorithm [19]. These modifications make our method more robust (a) to face the *feasibility* problem, and (b) to discover good solutions despite poor initial guesses. Our algorithm is

called control-limited Feasibility-driven Differential Dynamic Programming (FDDP) (in short Box-FDDP). It comprises two modes: *feasibility-driven* and *control-bounded* modes. Box-FDDP combines a hybridization of the multiple-shooting with DDP to leverage feasibility under control limits. In our results, we highlight the impact and importance of these changes over a wide range of different optimal control problems: from double pendulum to humanoid locomotion (Fig. 1).

The rest of the paper is organized as follows. In Section II, we quickly describe the optimal control formulation and then recall the DDP algorithm with control limits. Section III describes our algorithm called Box-FDDP. Results that support the impact and importance of our proposed changes are provided for several optimal control problems in Section IV, and Section V summarizes the work conclusions.

II. PRELIMINARIES

In this section, we give a short introduction to the Box-DDP algorithm (Section II-A); necessary for our proposed algorithm called Box-FDDP; for a complete description see [29], [12].

A. Differential dynamic programming with control-limits

As proposed by [12], the control-limited DDP locally approximates the optimal flow (i.e. the Value function) as

$$V_k(\delta \mathbf{x}_k) = \min_{\delta \mathbf{u}_k} l_k(\delta \mathbf{x}_k, \delta \mathbf{u}_k) + V_{k+1}(\mathbf{f}_k(\delta \mathbf{x}_k, \delta \mathbf{u}_k)), \quad (1)$$

$$\text{s.t.} \quad \underline{\mathbf{u}} \leq \mathbf{u}_k + \delta \mathbf{u}_k \leq \bar{\mathbf{u}},$$

which breaks the constrained Optimal Control (OC) problem into a sequence of simpler sub-problems; $\underline{\mathbf{u}}, \bar{\mathbf{u}}$ are the lower and upper bounds of the control, respectively. Then, a local search direction is computed through a Linear Quadratic (LQ) approximation of the Value function:

$$\delta \mathbf{u}_k^*(\delta \mathbf{x}_k) = \arg \min_{\delta \mathbf{u}_k} \frac{1}{2} \begin{bmatrix} 1 \\ \delta \mathbf{x}_k \\ \delta \mathbf{u}_k \end{bmatrix}^T \overbrace{\begin{bmatrix} 0 & \mathbf{Q}_{\mathbf{x}\mathbf{x}_k}^T & \mathbf{Q}_{\mathbf{x}\mathbf{u}_k}^T \\ \mathbf{Q}_{\mathbf{x}_k} & \mathbf{Q}_{\mathbf{x}\mathbf{x}_k} & \mathbf{Q}_{\mathbf{x}\mathbf{u}_k} \\ \mathbf{Q}_{\mathbf{u}_k} & \mathbf{Q}_{\mathbf{x}\mathbf{u}_k}^T & \mathbf{Q}_{\mathbf{u}\mathbf{u}_k} \end{bmatrix}}^{\mathbf{H}(\delta \mathbf{x}_k, \delta \mathbf{u}_k, \bar{V}_k, k)} \begin{bmatrix} 1 \\ \delta \mathbf{x}_k \\ \delta \mathbf{u}_k \end{bmatrix}, \quad (2)$$

$$\text{s.t.} \quad \underline{\mathbf{u}} \leq \mathbf{u}_k + \delta \mathbf{u}_k \leq \bar{\mathbf{u}}, \quad (3)$$

where the \mathbf{Q}_k terms represent the LQ approximation of the Hamiltonian function $\mathbf{H}(\cdot)$, and the derivatives of Value function $\bar{V}_k = (V_{\mathbf{x}_k}, V_{\mathbf{x}\mathbf{x}_k})$ take the role of the costate variables. From the derivatives of the cost and dynamics functions $l_k(\cdot)$, $\mathbf{f}_k(\cdot)$, the Hamiltonian is calculated around a guess $(\mathbf{x}_k^i, \mathbf{u}_k^i)$ at each i -th iteration [29]. Solving Eq. (2) provides the feed-forward term \mathbf{k}_k and the feedback gain \mathbf{K}_k at each discretization point k .

1) *Control-bounded direction*: Due to the mathematical simplicity of the control bounds, a subspace minimization approach allows the active set to change rapidly [25]. The subspace is defined by the search direction projected onto the feasible box. To adopt this strategy into DDP algorithm, Tassa et al. [19] proposed to break the problem into feed-forward

²In the following section we describe formally the control Hamiltonian.

³For more details about direct collocation see [26].

and feedback sub-problems, where the feed-forward problem is defined as

$$\begin{aligned} \mathbf{k}_k &= \arg \min_{\delta \mathbf{u}_k} \frac{1}{2} \delta \mathbf{u}_k^T \mathbf{Q}_{\mathbf{u}\mathbf{u}_k} \delta \mathbf{u}_k + \mathbf{Q}_{\mathbf{u}_k}^T \delta \mathbf{u}_k, \\ \text{s.t.} \quad & \mathbf{u} \leq \mathbf{u}_k + \delta \mathbf{u}_k \leq \bar{\mathbf{u}}, \end{aligned} \quad (4)$$

and it is solved by iteratively identifying the active set and then moving along the free subspace of the Newton step (i.e. Projected-Newton QP [30]). Instead, the feedback gain is computed along the free subspace of the Hessian, i.e.

$$\mathbf{K}_k = -\mathbf{Q}_{\mathbf{u}\mathbf{u},f_k}^{-1} \mathbf{Q}_{\mathbf{u}\mathbf{x}_k}, \quad (5)$$

where $\mathbf{Q}_{\mathbf{u}\mathbf{u},f_k}^{-1}$ is the control Hessian of the free subspace, and it is computed from feed-forward sub-problem. Note that the Box-QP computes the Newton direction along the free subspace.

With this feedback gain, the changes in the nominal trajectory are projected onto the feasible box. Additionally, the Box-QP algorithm requires a feasible warm-start $\delta \mathbf{u}_k^0$, and if it has the same active set, then the solution is calculated within a single iteration⁴.

III. CONTROL-LIMITED FDDP

The Box-FDDP comprises two modes: *feasibility-driven* and *control-bounded* modes, that might be chosen in a given iteration (Algorithm 1). The feasibility-driven mode uses a DDP hybridization of the multiple-shooting formulation to compute the search direction and step length (lines 7 and 15). Instead, the control-bounded mode projects the search direction onto the feasible control region whenever the dynamics constraint is feasible (line 10). Additionally, the applied control is always projected onto its feasible box (line 13), causing dynamic-infeasible iterations to reach the control box. Technical descriptions of both modes are elaborated in Sections III-A and III-B.

A. Search direction of Box-FDDP

In direct multiple-shooting, the nonlinearities of the dynamics are distributed over the entire horizon, instead of being accumulated as in single shooting [31]. In DDP, the feedback gain helps to distribute the dynamics nonlinearities as well. However, it does not resemble the Hamilton-Jacobi-Bellman (HJB) equation applied to a direct multiple-shooting formulation as described below.

1) *Computing the gaps:* Given a current iterate $(\mathbf{x}_s, \mathbf{u}_s)$, we compute the gaps by performing a nonlinear rollout, i.e.

$$\bar{\mathbf{f}}_{k+1} = \mathbf{f}(\mathbf{x}_k, \mathbf{u}_k) - \mathbf{x}_{k+1}, \quad (6)$$

where $\mathbf{f}(\mathbf{x}_k, \mathbf{u}_k)$ is the rollout state at interval $k+1$, and \mathbf{x}_{k+1} is the next shooting state.

In the standard Box-DDP, an initial forward pass is performed in order to close the gaps. Instead, our Box-FDDP computes the gaps once at each iteration (line 3), and then uses them to find the search direction (Section III-A3) and to compute the expected improvement (Section III-B4).

⁴The computational cost of a single iteration is similar to performing a Cholesky decomposition.

Algorithm 1: Control-limited FDDP (Box-FDDP)

```

1 compute LQ approximation of the cost and dynamics
2 if infeasible iterate then
3   compute the gaps, Eq. (6)
4 for  $k \leftarrow N-1$  to 0 do
5   update the feasibility-driven Hamiltonian, Eq. (9)
6   if infeasible iterate then
7     compute feasibility-driven direction, Eq. (11)
8   else
9     clamp Box-QP warm-start, Eq. (12)
10    compute control-bounded direction, Eq. (4)-(5)
11 for  $\alpha \in \{1, \frac{1}{2}, \dots, \frac{1}{2^n}\}$  do
12   for  $k \leftarrow 0$  to  $N$  do
13     project control onto the feasible box, Eq. (13)
14     if infeasible iterate or  $\alpha \neq 1$  then
15       update the gaps, Eq. (14)
16     else
17       close the gaps,
18        $\mathbf{f}_k = \mathbf{0} \ \forall k \in \{0, \dots, N-1\}$ 
19     perform step, Eq. (16)
20   compute the expected improvement, Eq. (17)
21   if success step then
22     break

```

2) Hamiltonian of direct multiple-shooting formulation:

Without loss of generality, we use the GN approximation [16] to write the Hamiltonian function as

$$\begin{aligned} \mathbf{H}(\cdot) &= \frac{1}{2} \begin{bmatrix} 1 \\ \delta \mathbf{x}_{k+1} \end{bmatrix}^T \begin{bmatrix} 0 & \mathbf{V}_{\mathbf{x}_{k+1}}^T \\ \mathbf{V}_{\mathbf{x}_{k+1}} & \mathbf{V}_{\mathbf{x}\mathbf{x}_{k+1}} \end{bmatrix} \begin{bmatrix} 1 \\ \delta \mathbf{x}_{k+1} \end{bmatrix} \\ &+ \frac{1}{2} \begin{bmatrix} 1 \\ \delta \mathbf{x}_k \\ \delta \mathbf{u}_k \end{bmatrix}^T \begin{bmatrix} 0 & \mathbf{l}_{\mathbf{x}_k}^T & \mathbf{l}_{\mathbf{u}_k}^T \\ \mathbf{l}_{\mathbf{x}_k} & \mathbf{l}_{\mathbf{x}\mathbf{x}_k} & \mathbf{l}_{\mathbf{x}\mathbf{u}_k} \\ \mathbf{l}_{\mathbf{u}_k} & \mathbf{l}_{\mathbf{x}\mathbf{u}_k}^T & \mathbf{l}_{\mathbf{u}\mathbf{u}_k} \end{bmatrix} \begin{bmatrix} 1 \\ \delta \mathbf{x}_k \\ \delta \mathbf{u}_k \end{bmatrix}, \quad (7) \end{aligned}$$

where $\mathbf{l}_{\mathbf{x}}, \mathbf{l}_{\mathbf{u}}$ and $\mathbf{l}_{\mathbf{x}\mathbf{x}}, \mathbf{l}_{\mathbf{x}\mathbf{u}}, \mathbf{l}_{\mathbf{u}\mathbf{u}}$ are the gradient and Hessian of the cost function, respectively, $\delta \mathbf{x}_{k+1} = \mathbf{f}_{\mathbf{x}_k} \delta \mathbf{x}_k + \mathbf{f}_{\mathbf{u}_k} \delta \mathbf{u}_k$ is the linearized dynamics, and $\mathbf{f}_{\mathbf{x}}, \mathbf{f}_{\mathbf{u}}$ are its Jacobians. However, in a direct multiple-shooting setting, we have a drift in the linearized dynamics

$$\delta \mathbf{x}_{k+1} = \mathbf{f}_{\mathbf{x}_k} \delta \mathbf{x}_k + \mathbf{f}_{\mathbf{u}_k} \delta \mathbf{u}_k + \bar{\mathbf{f}}_{k+1} \quad (8)$$

due to the gaps $\bar{\mathbf{f}}_{k+1}$ produced between multiple-shoots. Then, according to the PMP, the Riccati recursion needs to be adapted as follows:

$$\begin{aligned} \mathbf{Q}_{\mathbf{x}_k} &= \mathbf{l}_{\mathbf{x}_k} + \mathbf{f}_{\mathbf{x}_k}^T \mathbf{V}_{\mathbf{x}_{k+1}}^+, \\ \mathbf{Q}_{\mathbf{u}_k} &= \mathbf{l}_{\mathbf{u}_k} + \mathbf{f}_{\mathbf{u}_k}^T \mathbf{V}_{\mathbf{x}_{k+1}}^+, \\ \mathbf{Q}_{\mathbf{x}\mathbf{x}_k} &= \mathbf{l}_{\mathbf{x}\mathbf{x}_k} + \mathbf{f}_{\mathbf{x}_k}^T \mathbf{V}_{\mathbf{x}\mathbf{x}_{k+1}} \mathbf{f}_{\mathbf{x}_k}, \\ \mathbf{Q}_{\mathbf{x}\mathbf{u}_k} &= \mathbf{l}_{\mathbf{x}\mathbf{u}_k} + \mathbf{f}_{\mathbf{x}_k}^T \mathbf{V}_{\mathbf{x}\mathbf{x}_{k+1}} \mathbf{f}_{\mathbf{u}_k}, \\ \mathbf{Q}_{\mathbf{u}\mathbf{u}_k} &= \mathbf{l}_{\mathbf{u}\mathbf{u}_k} + \mathbf{f}_{\mathbf{u}_k}^T \mathbf{V}_{\mathbf{x}\mathbf{x}_{k+1}} \mathbf{f}_{\mathbf{u}_k}, \end{aligned} \quad (9)$$

where

$$\mathbf{V}_{\mathbf{x}_{k+1}}^+ = \mathbf{V}_{\mathbf{x}_{k+1}} + \mathbf{V}_{\mathbf{x}\mathbf{x}_{k+1}} \bar{\mathbf{f}}_{k+1} \quad (10)$$

is the Jacobian of the Value function after the deflection produced by $\bar{\mathbf{f}}_{k+1}$, and the Hessian of the Value function remains unchanged. Indeed, this is possible since DDP approximates the Value function to a LQ model. Note that a similar derivation is proposed by [17].

3) *Feasibility-driven direction*: During *dynamic-infeasible* iterates (line 7), we compute a *control-unbounded* direction⁵:

$$\begin{aligned} \mathbf{k}_k &= -\mathbf{Q}_{\mathbf{u}\mathbf{u}_k}^{-1} \mathbf{Q}_{\mathbf{u}_k}, \\ \mathbf{K}_k &= -\mathbf{Q}_{\mathbf{u}\mathbf{u}_k}^{-1} \mathbf{Q}_{\mathbf{u}\mathbf{x}_k}. \end{aligned} \quad (11)$$

The reason is due to the fact that we cannot quantify the effect of the gaps on the control bounds, which are needed to solve the feed-forward sub-problem Eq. (4). Note that our approach is equivalent to opening the control bounds during dynamic-infeasible iterates.

4) *Control-bounded direction*: We warm-start the Box-QP using the feed-forward term \mathbf{k}_k computed in the previous iteration. However, in case of a previous infeasible iteration, \mathbf{k}_k might fall outside the feasible box (i.e. $\bar{\mathbf{u}} - \delta \mathbf{u}_k \leq \mathbf{k}_k \leq \underline{\mathbf{u}} - \delta \mathbf{u}_k$). This is in contrast to the standard Box-DDP, in which a feasible warm-start \mathbf{u}_s^0 needs to be provided, and then, the iterates always remain feasible.

To handle infeasible iterates, we propose to clamp the warm-start of the Box-QP (line 9) as

$$\llbracket \mathbf{k}_k \rrbracket_{\mathbf{u}-\delta \mathbf{u}_k} = \min(\max(\mathbf{k}_k, \bar{\mathbf{u}} - \delta \mathbf{u}_k), \underline{\mathbf{u}} - \delta \mathbf{u}_k), \quad (12)$$

where $\bar{\mathbf{u}} - \delta \mathbf{u}_k$ and $\underline{\mathbf{u}} - \delta \mathbf{u}_k$ are the upper and lower bounds of the feed-forward sub-problem, Eq. (4), respectively.

5) *Regularization*: Each time that the computation of the feed-forward sub-problem fails, Eq. (4), we increment the regularization over $\mathbf{Q}_{\mathbf{u}\mathbf{u}}$ and re-start the computation of the direction. On the other hand, each time that the algorithm accepts a big step⁶, then we decrease the regularization. With this, we provide major robustness to the algorithm since it moves from Newton direction to steepest-descent, or vice versa.

B. Step-length of Box-FDDP

As far as we know, Tassa et al. [12] proposed only to modify the search direction using a Box-QP. However, it is important to pay attention to the rollout as well, during which we find a step length that minimizes the cost [25]. A similar motivation can be found in methods such as [22], [23], where a standard line-search procedure is used around a local model.

1) *Projecting the rollout towards the feasible box*: We propose to project the control onto the feasible box in the nonlinear rollout (line 13), i.e.

$$\hat{\mathbf{u}}_k \leftarrow \min(\max(\hat{\mathbf{u}}_k, \bar{\mathbf{u}}), \underline{\mathbf{u}}), \quad (13)$$

where $\hat{\mathbf{u}}_k$ is the control policy computed from the search direction; for more details see Section III-B3. Our method does not require to solve another QP problem [22] or to project the linear search direction given the gaps on the dynamics [23].

⁵In this work, with *control-unbounded* direction, we also refer to feasibility-driven direction, i.e., the direction ignoring the control constraints.

⁶Steps with $\alpha \geq \alpha_0$, where α_0 is an user-defined threshold.

2) *Updating the gaps*: In related work [18] is analyzed the behavior of the gaps during the numerical optimization, i.e. by iteratively solving the Karush-Kuhn-Tucker (KKT) problem of a direct multiple-shooting algorithm. Their conclusion is that the gaps will be either partially closed by a factor of

$$\bar{\mathbf{f}}_k \leftarrow (1 - \alpha) \bar{\mathbf{f}}_k, \quad (14)$$

where α is the accepted step-length found by the line-search procedure (line 11-21), or completely closed in case of a full-step ($\alpha = 1$).

3) *Nonlinear step*: With a nonlinear rollout⁷ (line 18), we avoid the linear prediction error of the dynamics that is typically handled by a *merit* function in off-the-shelf NLP solvers. Therefore, the prediction of gaps after applying an α -step are:

$$\begin{aligned} \bar{\mathbf{f}}_{k+1}^{i+1} &= \bar{\mathbf{f}}_{k+1}^i - \alpha(\delta \mathbf{x}_{k+1} - \mathbf{f}_{\mathbf{x}_k} \delta \mathbf{x}_k - \mathbf{f}_{\mathbf{u}_k} \delta \mathbf{u}_k) \\ &= (1 - \alpha)(\mathbf{f}(\mathbf{x}_k, \mathbf{u}_k) - \mathbf{x}_{k+1}), \end{aligned} \quad (15)$$

and if we keep the gap-contraction rate of Eq. (14), then we obtain

$$\begin{aligned} \hat{\mathbf{x}}_k &= \mathbf{f}(\hat{\mathbf{x}}_{k-1}, \hat{\mathbf{u}}_{k-1}) - (1 - \alpha) \bar{\mathbf{f}}_{k-1}, \\ \hat{\mathbf{u}}_k &= \mathbf{u}_k + \alpha \mathbf{k}_k + \mathbf{K}_k(\hat{\mathbf{x}}_k - \mathbf{x}_k), \end{aligned} \quad (16)$$

where \mathbf{k}_k and \mathbf{K}_k are the feed-forward term and feedback gains computed by Eq. (11) or Eq. (4)-(5), and the initial condition of the rollout is defined as $\hat{\mathbf{x}}_0 = \tilde{\mathbf{x}}_0 - (1 - \alpha) \bar{\mathbf{f}}_0$. This is in contrast to the standard Box-DDP, in which the gaps are always closed.

4) *Expected improvement*: It is critical to properly evaluate the success of a trial step. Given the current gaps on the dynamics $\bar{\mathbf{f}}_k$, the Box-FDDP computes the expected improvement of a computed search direction as

$$\Delta J(\alpha) = \Delta_1 \alpha + \frac{1}{2} \Delta_2 \alpha^2, \quad (17)$$

with

$$\begin{aligned} \Delta_1 &= \sum_{k=0}^N \mathbf{k}_k^\top \mathbf{Q}_{\mathbf{u}_k} + \bar{\mathbf{f}}_k^\top (V_{\mathbf{x}_k} - V_{\mathbf{x}\mathbf{x}_k} \hat{\mathbf{x}}_k), \\ \Delta_2 &= \sum_{k=0}^N \mathbf{k}_k^\top \mathbf{Q}_{\mathbf{u}\mathbf{u}_k} \mathbf{k}_k + \bar{\mathbf{f}}_k^\top (2V_{\mathbf{x}\mathbf{x}_k} \mathbf{x}_k - V_{\mathbf{x}\mathbf{x}_k} \bar{\mathbf{f}}_k). \end{aligned} \quad (18)$$

Note that J is the total of cost of a given state-control trajectory $(\mathbf{x}_s, \mathbf{u}_s)$.

We obtain this expression by computing the cost from a linear rollout of the current control policy as described in Eq. (16). Finally, we also accept ascend directions since we use the Goldstein condition to check for the trial step.

IV. RESULTS

Box-FDDP outperforms Box-DDP on a wide number of optimal control problems which are described in Section IV-A. In Section IV-B, we provide a comparison that shows the advantages of the proposed modifications. Later, we analyze the gap contraction and how it is connected with the dynamic

⁷In this work, *rollout* is sometimes referred as nonlinear step.

nonlinearities (Section IV-B2). Finally, we show that the early control saturation of the Box-DDP has disadvantages (Section IV-C).

A. Optimal control problems

We compare the performance of our solver against Box-DDP [19] for a range of different OC problems: an under-actuated double pendulum, a quadcopter navigating through a narrow passage and looping, various gaits in legged locomotion, aggressive jumps and unstable hopping, and whole-body manipulation and balance. All the studied cases highlight the benefits of our proposed method: Box-FDDP. To make a fair comparison, we use the same initial regularization value (10^{-9}) and stopping criteria. Fig. 2 shows snapshots of motion computed for some of these problems, for more details see the accompanying video⁸. The Box-FDDP solver and examples are publically available in [32].

1) *Double pendulum (pend)*: The goal is to swing from the stable to the unstable equilibrium points, i.e. from down-ward to up-ward positions, respectively. To increase the problem complexity, the double pendulum (with weight of ≈ 4.5 N) has a single actuated joint with small range of control (from -5 to 5 N, largely insufficient for a static execution of the trajectory). The time horizon is 1 s with 100 nodes. We define a quadratic cost function, for each node, that aims to reach the up-ward position. For the running and terminal nodes, we use the weight values of 10^{-4} and 10^4 , respectively. Additionally, we provide state and control regularization terms. To test the solver capabilities, we do not provide an initial guess, thus the swing-up strategy is discovered by the solver itself. Finally, we implement the cost, dynamics and their analytical derivatives using Python.

2) *Quadcopter*: We consider three tasks for the IRIS quadcopter: reaching goal (quad), looping maneuver (loop), and traversing a narrow passage (narrow). We define different way-points to describe the tasks, where each way-point specifies the desired pose and velocity. The way-points are described through cost functions in the robot placement and velocity. These cost functions are quadratic term with 10^2 and 100 as weight values for the running and terminal nodes, respectively. The vehicle pose is described as $\mathbb{SE}(3)$ element, which allows us to consider any kind of motion such as *looping* maneuvers. Control inputs are considered to be the thrust produced by the propellers, which can vary within a range from 0.1 to 10.3 N each. We compute the dynamics using the Articulated Body Algorithm (ABA) algorithm⁹, the analytical derivatives are calculated as described in [34]. We integrate the dynamics with step time of 30^{-2} s. The solution is computed from a cold-start of the solver.

3) *Aggressive jump, unstable hopping, and various gaits*: We use the ANYmal quadruped robot to generate a wide range of motions — jumping, hopping, walking, trotting, pacing, and bounding. We deliberately reduce the torque and velocity limits to 32 N m and 7.5 rad/s, respectively. The joint velocity limits make it particularly hard to solve the jumping task

(jump). Finally, the unstable hopping task (hop) is described with a long horizon: 5.8 s with 580 nodes. It includes 10 hops in total with a phase that switches the feet in contact. We define quadratic terms, with a weight value of 10^6 , to track the desired swing-foot placements. We use a quadratic barrier to penalize the joint velocities and the contact forces that are outside the limits. We regularization the state trajectory around the default robot's configuration. For all the experiments, we use a friction coefficient of 0.7. Furthermore, we use the multi-phase rigid contact dynamics and their analytical derivatives as described in [35], [18], respectively. During a contact transition, we employ the impulse dynamics with analytical derivatives. On the other hand, we warm-start the solver using the default posture and the quasi-static torques for each node of the initial guess trajectories. The default posture defines the standing position of the robot; it does not provide any relevant information for a specific maneuver (e.g. jump). The quasic static torques describe the gravity effect subject to the robot's default posture. However, we have observed that omitting to warm start the controls (i.e. \mathbf{u}_s^0) would not affect the solver performance.

4) *Whole-body manipulation and balance*: We consider three problems for the Talos humanoid robot: whole-body manipulation (man), hand control while balancing in single leg (taichi), and a monkey bar task (bar). For the monkey bar task, we increase by 10 times the joint torque limits of the arms¹⁰. Additionally, we consider joint position limits in each scenario. Both taichi and monkey bar tasks are divided in three phases; for the taichi task: manipulation, standing on one foot, and balancing; for the monkey bar task: grasping the bar, climbing up, and landing on ground. We do not include friction cone constraints in the grasping bar phase for the hands. We use the contact-placement cost functions for both: feet and hands, regularization terms, and dynamics as described for the ANYmal case. Finally, we use the same warm-start strategy used the ANYmal problems. For the details about the ANYmal problems see above (Section IV-A3).

B. Advantages of the feasibility mode

To understand the benefits of the feasibility-mode, we analyze the resulting total cost and number of iterations for both: Box-FDDP and Box-DDP. As shown in Fig. 3, Box-FDDP's solutions (*-feas) have lower total cost and are computed with fewer iterations when compared to Box-DDP. We use the same warm-start strategy for both solvers as described above. We summarize the results of each benchmark problem in Table I.

1) *Greater globalization strategy*: The feasibility-driven mode becomes crucial to solve the double pendulum (pend), monkey bar task (bar), aggressive jumping (jump), and unstable hopping (hop) problems, in which the Box-DDP fails to find a solution (Table I). This mode helps to find a feasible sequence of controls despite the poor initialization warm-start. Indeed, infeasible iterations can be seen as a globalization strategy that ensure convergence from remote initial points as they balance objective and feasibility. We encountered that this trade-off could also improve the solution. For instance,

⁸<https://youtu.be/ITbUXqxsBM>

⁹For more details about the ABA algorithm see [33].

¹⁰Talos' arms are not strong enough to support its own weight.

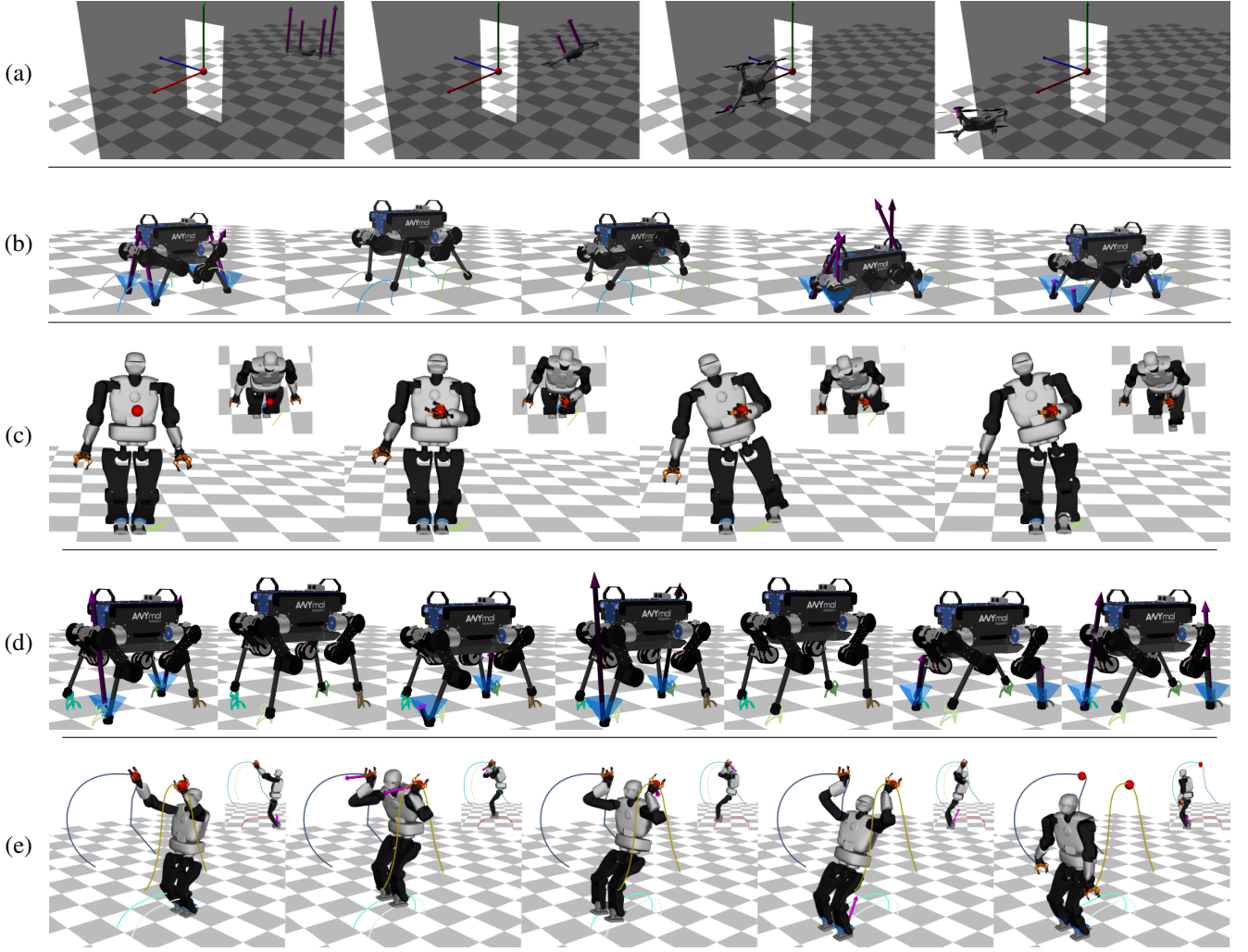


Fig. 2. Snapshots of generated robot maneuvers using Box-FDDP. (a) traversing a narrow passage with a quadcopter (quad); (b) aggressive jumping of 30 cm that reaches ANYmal limits (jump); (c) Talos balancing on a single leg (taichi); (d) ANYmal hopping with two legs (hop); (e) Talos climbing in a monkey bar.

TABLE I
NUMBER OF ITERATIONS, TOTAL COST, AND SOLUTION SUCCESS RATE.

| Problems | Box-DDP | | | Box-FDDP (feas) | | |
|-------------|---------|--------------------|------|-----------------|--------------------|------|
| | Iter. | Cost | Sol. | Iter. | Cost | Sol. |
| pend | 424 | 0.223 | ✗ | 31 | 0.0273 | ✓ |
| quad-goal | 23 | 0.0764 | ✓ | 18 | 0.0072 | ✓ |
| quad-loop | 133 | 6.7211 | ✓ | 56 | 0.6444 | ✓ |
| quad-narrow | 70 | 1.9492 | ✓ | 35 | 0.4577 | ✓ |
| man | 72 | 4.6193 | ✓ | 65 | 4.6193 | ✓ |
| taichi | 148 | 6.8184 | ✓ | 140 | 6.8184 | ✓ |
| jump | 646 | 7.21×10^4 | ✗ | 454 | 1.81×10^4 | ✓ |
| hop | 18 | 1.13×10^6 | ✗ | 205 | 2.23×10^4 | ✓ |
| bar | 27 | 927.7 | ✗ | 358 | 23.316 | ✓ |

✓ solver finds a solution, ✗ solver does not find a solution.

early clamping of control commands (produced by Box-DDP) generates unnecessary loops during the quadcopter navigation.

2) *Gap contraction and nonlinearities*: Fig. 4 shows the gap contraction for each benchmark problem. We observe that the gap contraction rate is highly influenced by the nonlinearities of the system's dynamics. When compared to the dynamics, the nonlinearities of the task have a smaller effect (e.g. jump vs hop). Note that the gap contraction speed

follows the order: humanoid, quadruped, double pendulum, and quadcopter.

Propagation errors due to the dynamics linearization have an important influence on the algorithm progress, mainly because DDP-based methods maintain a local quadratic approximation of the Value function. In other words, the prediction of the expected improvement is more accurate for systems with less nonlinearities and, as a result, the algorithm tends to accept bigger steps that result in higher gap reductions.

While the gaps are open, our algorithm is in feasibility-driven mode. During this phase, the cost reduction is smaller than in the control-bounded mode, in particular for very nonlinear systems (see Fig. 3 and 4). However, once the gaps are closed, a higher cost reductions often appear in very nonlinear systems.

3) *Highly-dynamic maneuvers*: Our algorithm can solve a wide range of motions: from unstable and consecutive hops to aggressive and constrained jumps. In Fig. 5, we show the joint torques and velocities of a single leg for the ANYmal's jumping task (depicted in Fig. 2-b). The motion consists of three phases: jumping (0 - 300 ms), flying (300 - 700 ms),

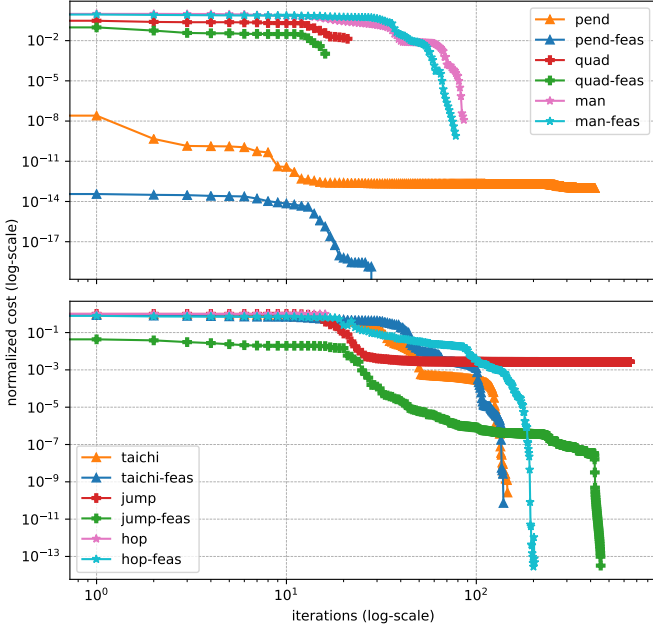


Fig. 3. Cost and convergence comparison for different optimal control problems. The Box-FDDP outperforms the Box-DDP in all the cases: (top) double pendulum (pend), quadcopter navigation (quad), and whole-body manipulation (man); and (bottom) whole-body balance (taichi), quadrupedal jumping (jump), quadrupedal hopping (hop). Box-FDDP (*)-feas solves the problem with fewer iterations and lower cost than Box-DDP. Furthermore, Box-DDP fails to solve the hardest problems: i.e. double pendulum, quadrupedal jumping, and hopping. Our algorithm shows better globalization strategy, i.e. it is less sensitive to poor initialization compared with Box-DDP.

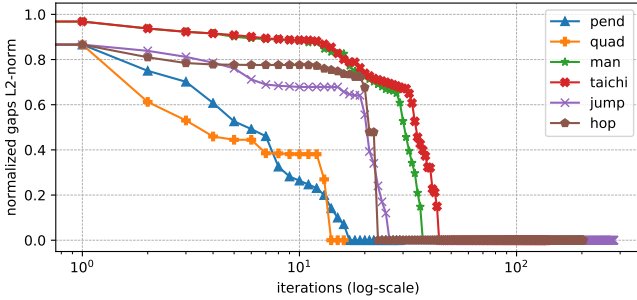


Fig. 4. Gap contraction of Box-FDDP for different optimal control problems. For all the cases, the gaps are open for the first several iterations. The gap contraction rate varies according to the accepted step-length. Smaller contraction rates, during the first iterations, appear in very nonlinear problems (taichi, man, hop, and jump), because of the larger error of the search direction.

and landing (700 - 1000 ms). We reduced the real joint limits of the ANYmal robot: from 40 to 32 N m (torque limits) and from 15 to 7.5 rad/s (velocity limits). Thus, generating a 30 cm jump becomes a very challenging task. The constraint violations on the state limits appear due to the fact that we use quadratic penalization to enforce them. Nonetheless, we only encountered these violations in very constrained problems.

For the walking, trotting, pacing, and bounding gaits (reporting in the accompanying video), the Box-FDDP converges approximately with the same number of iterations achieved by the DDP solver (i.e. unconstrained case).

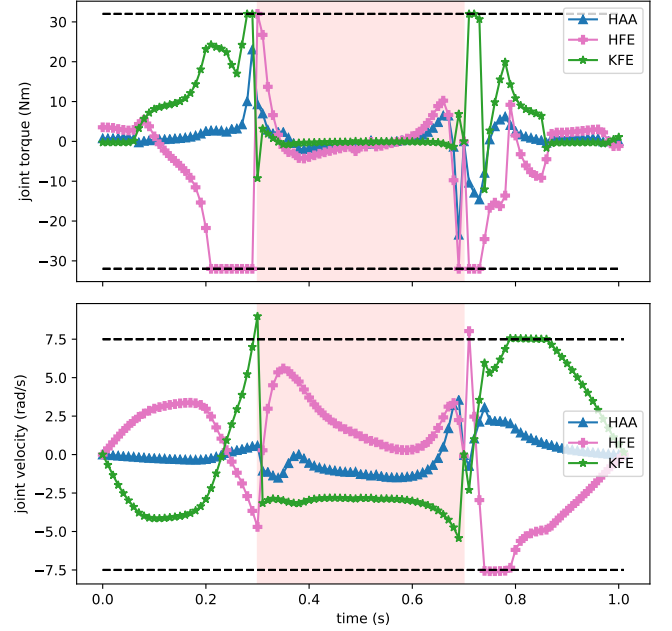


Fig. 5. Joint torques and velocity for the ANYmal jumping maneuver. (top) Generated torques of the LF joints and its limits (32 N m); (bottom) Generated velocities of the LF joint and its limits (7.5 rad/s). The red region describes the flight phase. Note that HAA, HFE, and KFE are the abduction/adduction, hip flexion/extension and knee flexion/extension joints, respectively.

C. Box-FDDP, Box-DDP, and squashing approach in nonlinear problems

We compare the performance of Box-FDDP, Box-DDP and DDP with a squashing function for three scenarios with the IRIS quadcopter: reaching goal (goal), looping maneuver (loop), and traversing a narrow passage (narrow). We use a sigmoidal element-wise squashing function of the form:

$$s^i(\mathbf{u}^i) = \frac{1}{2} \left(\frac{\mathbf{u}^i + \sqrt{\beta^2 + (\mathbf{u}^i - \underline{\mathbf{u}}^i)^2}}{\beta} + \frac{\mathbf{u}^i - \sqrt{\beta^2 + (\mathbf{u}^i - \bar{\mathbf{u}}^i)^2}}{\beta} \right),$$

in which the sigmoid is approximated through two smooth-abs functions, β defines its smoothness, and $\underline{\mathbf{u}}^i$, $\bar{\mathbf{u}}^i$ are the element-wise lower and upper control bounds, respectively. We introduce this squashing function on the system controls as: $\mathbf{x}_{k+1} = \mathbf{f}(\mathbf{x}_k, \mathbf{s}(\mathbf{u}_k))$. We use $\beta = 2$ for all the experiments presented in this work.

Fig. 6 shows that Box-FDDP converges faster than the other approaches. Furthermore, the motions computed by Box-FDDP are more intuitive and with the lowest cost as reported in Table I and in accompanying video. We also observe that the squashing approach converges sooner compared to Box-DDP for the looping task. The main reason is due to the early saturation of the controls performed by Box-DDP.

In Fig. 7, we show the cost evolution for 10 different initial configurations of the reaching goal task. The target and initial configurations are $(3, 0, 1)$ and $(-0.3 \pm 0.6, 0, 0)$ m, respectively. Infeasible iterations, in Box-FDDP, produce a very low cost in the first iterations. The squashing approach is the most sensitive to initial conditions. However, on average,

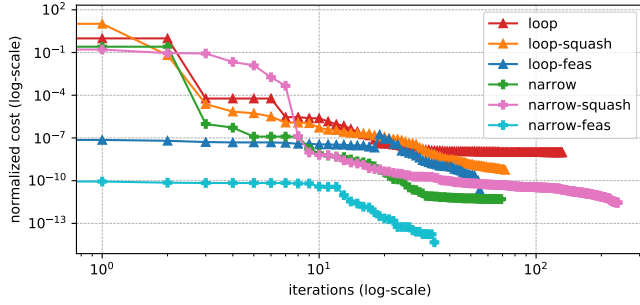


Fig. 6. Cost and convergence comparison for different quadcopter maneuvers: looping (loop) and narrow passage traversing (narrow). Box-FDDP (*-feas) outperforms both Box-DDP and DDP with squashing function (*-squash).

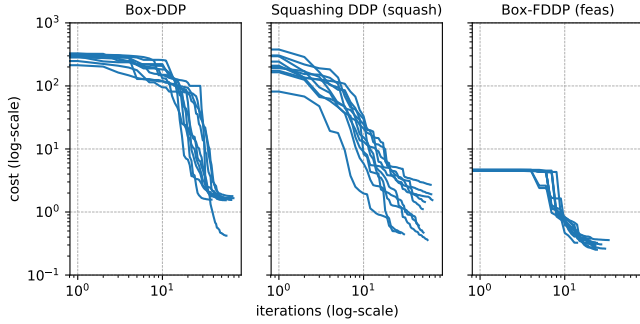


Fig. 7. Costs associated for 10 different initial configurations of reaching goal task. Box-FDDP converges earlier and with lower total cost than Box-DDP and DDP with squashing function. The performance of the squashing function approach exhibits a high dependency on the initial condition.

it produces slightly better solutions than Box-DDP. This is in contrast to the reported results in [19], where the performance was analyzed only for LQ optimal control problem.

V. CONCLUSION

In this paper, we proposed a direct-indirect hybridization of the control-limited DDP algorithm (Box-FDDP). Our method discovers good solutions despite poor initial guesses thanks to infeasible iterations, which resembles a direct multiple-shooting approach. A vast range of optimal control problems demonstrate the benefits of the proposed method. Future work will focus on general inequalities constraints and model predictive control. Our implementation of Box-FDDP including all examples will be available soon.

REFERENCES

- [1] J. T. Betts, *Practical Methods for Optimal Control and Estimation Using Nonlinear Programming*, 2nd ed. USA: Cambridge University Press, 2009.
- [2] P. E. Gill, W. Murray, and M. A. Saunders, "SNOPT: An SQP Algorithm for Large-Scale Constrained Optimization," *SIAM Rev.*, 2005.
- [3] R. H. Byrd, J. Nocedal, and R. A. Waltz, "KNITRO: An integrated package for nonlinear optimization," in *Large Scale Nonlinear Optimization*, 35–59, 2006.
- [4] A. Wächter and L. T. Biegler, "On the implementation of an interior-point filter line-search algorithm for large-scale nonlinear programming," *Mathematical Programming*, 2006.
- [5] P.-B. Wieber, "Trajectory Free Linear Model Predictive Control for Stable Walking in the Presence of Strong Perturbations," in *IEEE Int. Conf. Hum. Rob. (ICHR)*, 2006.
- [6] D. Pardo, L. Moller, M. Neunert, A. W. Winkler, and J. Buchli, "Evaluating Direct Transcription and Nonlinear Optimization Methods for Robot Motion Planning," *IEEE Robot. Automat. Lett. (RA-L)*, 2016.
- [7] J. Di Carlo, P. M. Wensing, B. Katz, G. Bledt, and S. Kim, "Dynamic Locomotion in the MIT Cheetah 3 Through Convex Model-Predictive Control," in *IEEE/RSJ Int. Conf. Intell. Rob. Sys. (IROS)*, 2018.
- [8] J. Carpentier, S. Tonneau, M. Naveau, O. Stasse, and N. Mansard, "A versatile and efficient pattern generator for generalized legged locomotion," in *IEEE Int. Conf. Rob. Autom. (ICRA)*, 2016.
- [9] C. Mastalli, M. Focchi, I. Havoutis, A. Radulescu, S. Calinon, J. Buchli, D. G. Caldwell, and C. Semini, "Trajectory and Foothold Optimization using Low-Dimensional Models for Rough Terrain Locomotion," in *IEEE Int. Conf. Rob. Autom. (ICRA)*, 2017.
- [10] B. Aceituno-Cabezas, C. Mastalli, H. Dai, M. Focchi, A. Radulescu, D. G. Caldwell, J. Cappelletto, J. C. Grieco, G. Fernandez-Lopez, and C. Semini, "Simultaneous Contact, Gait and Motion Planning for Robust Multi-Legged Locomotion via Mixed-Integer Convex Optimization," *IEEE Robot. Automat. Lett. (RA-L)*, 2017.
- [11] A. W. Winkler, D. C. Bellicoso, M. Hutter, and J. Buchli, "Gait and Trajectory Optimization for Legged Systems through Phase-based End-Effector Parameterization," *IEEE Robot. Automat. Lett. (RA-L)*, 2018.
- [12] Y. Tassa, T. Erez, and E. Todorov, "Synthesis and stabilization of complex behaviors through online trajectory optimization," in *IEEE/RSJ Int. Conf. Intell. Rob. Sys. (IROS)*, 2012.
- [13] J. Koenemann, A. Del Prete, Y. Tassa, E. Todorov, O. Stasse, M. Bennewitz, and N. Mansard, "Whole-body model-predictive control applied to the HRP-2 humanoid," in *IEEE/RSJ Int. Conf. Intell. Rob. Sys. (IROS)*, 2015.
- [14] M. Neunert, M. Stauble, M. Gifftthaler, C. D. Bellicoso, J. Carius, C. Gehring, M. Hutter, and J. Buchli, "Whole-Body Nonlinear Model Predictive Control Through Contacts for Quadrupeds," *IEEE Robot. Automat. Lett. (RA-L)*, 2018.
- [15] F. Farshidian, E. Jelavic, A. Satapathy, M. Gifftthaler, and J. Buchli, "Real-time motion planning of legged robots: A model predictive control approach," in *IEEE Int. Conf. Hum. Rob. (ICHR)*, 2017.
- [16] W. Li and E. Todorov, "Iterative Linear Quadratic Regulator Design for Nonlinear Biological Movement Systems," in *ICINCO*, 2004.
- [17] M. Gifftthaler, M. Neunert, M. Stauble, J. Buchli, and M. Diehl, "A Family of Iterative Gauss-Newton Shooting Methods for Nonlinear Optimal Control," in *IEEE/RSJ Int. Conf. Intell. Rob. Sys. (IROS)*, 2018.
- [18] C. Mastalli, R. Budhiraja, W. Merkt, G. Saurel, B. Hammoud, M. Naveau, J. Carpentier, L. Righetti, S. Vijayakumar, and N. Mansard, "Crocodyl: An Efficient and Versatile Framework for Multi-Contact Optimal Control," in *IEEE Int. Conf. Rob. Autom. (ICRA)*, 2020.
- [19] Y. Tassa, N. Mansard, and E. Todorov, "Control-Limited Differential Dynamic Programming," in *IEEE Int. Conf. Rob. Autom. (ICRA)*, 2014.
- [20] T. C. Lin and J. S. Arora, "Differential dynamic programming technique for constrained optimal control," in *Computational Mechanics*, 1991.
- [21] M. Gifftthaler and J. Buchli, "A Projection Approach to Equality Constrained Iterative Linear Quadratic Optimal Control," in *IEEE Int. Conf. Hum. Rob. (ICHR)*, 2017.
- [22] Z. Xie, C. K. Liu, and K. Hauser, "Differential dynamic programming with nonlinear constraints," in *IEEE Int. Conf. Rob. Autom. (ICRA)*, 2017.
- [23] T. A. Howell, B. Jackson, and Z. Manchester, "ALTRO: A Fast Solver for Constrained Trajectory Optimization," in *IEEE/RSJ Int. Conf. Intell. Rob. Sys. (IROS)*, 2019.
- [24] J. Albersmeyer and M. Diehl, "The Lifted Newton Method and Its Application in Optimization," *SIAM J. on Optimization*, 2010.
- [25] J. Nocedal and S. J. Wright, *Numerical Optimization*, 2nd ed. New York, NY, USA: Springer, 2006.
- [26] C. R. Hargraves and S. W. Paris, "Direct trajectory optimization using nonlinear programming and collocation," vol. 10, no. 4, 1987.
- [27] G. Lantoine and R. Russell, "A Hybrid Differential Dynamic Programming Algorithm for Robust Low-Thrust Optimization," 2008.
- [28] J. Marti-Saumell, J. Sola, C. Mastalli, and A. Santamaria-Navarro, "Squash-Box Feasibility Driven Differential Dynamic Programming," in *IEEE/RSJ Int. Conf. Intell. Rob. Sys. (IROS)*, 2020.
- [29] D. Mayne, "A second-order gradient method for determining optimal trajectories of non-linear discrete-time systems," *International Journal of Control*, 1966.
- [30] D. P. Bertsekas, "Projected newton methods for optimization problems with simple constraints," *SIAM Journal on Control and Optimization*, 1982.
- [31] M. Diehl, H. G. Bock, H. Diedam, and P.-B. Wieber, "Fast Direct Multiple Shooting Algorithms for Optimal Robot Control," in *Proc. Fast Motions in Biomechanics Robot*. Springer Berlin Heidelberg, 2006.

- [32] C. Mastalli, R. Budhiraja, and N. Mansard, “Crocodyl: a fast and flexible optimal control library for robot control under contact sequence,” <https://github.com/loco-3d/crocodyl>, 2019.
- [33] R. Featherstone, *Rigid Body Dynamics Algorithms*. Berlin, Heidelberg: Springer-Verlag, 2007.
- [34] J. Carpentier and N. Mansard, “Analytical Derivatives of Rigid Body Dynamics Algorithms,” in *Robotics: Science and Systems (RSS)*, 2018.
- [35] R. Budhiraja, J. Carpentier, C. Mastalli, and N. Mansard, “Differential Dynamic Programming for Multi-Phase Rigid Contact Dynamics,” in *IEEE Int. Conf. Hum. Rob. (ICHR)*, 2018.



Carlos Mastalli received the M.Sc. degree in mechatronics engineering from the Simón Bolívar University, Caracas, Venezuela, in 2013 and the Ph.D. degree in bio-engineering and robotics from the Istituto Italiano di Tecnologia, Genoa, Italy, in 2017.

He is currently a Research Associate in the University of Edinburgh with Alan Turing fellowship, Edinburgh, U.K. with S. Vijayakumar. From 2017 to 2019, he was a Postdoctoral Researcher in the Gepetto Team at LAAS-CNRS, Toulouse, France, working with N. Mansard and O. Stasse. Previously, he completed his Ph.D. on “Planning and Execution of Dynamic Whole-Body Locomotion on Challenging Terrain” under the supervision of I. Havoutis, C. Semini and D. G. Caldwell. He was Invited Researcher in the Eidgenössische Technische Hochschule Zürich, Zurich, Switzerland, with J. Buchli in 2016. His research combines the formalism of model-base approach with the exploration of vast robot’s data for legged robotics. He has contributions in optimal control, motion planning, whole-body control and machine learning for legged locomotion.



Worf Merkt received the BEng. degree in mechanical engineering with management and the Ph.D and M.Sc. degrees in robotics and autonomous systems from the University of Edinburgh, Edinburgh, U.K, in 2014, 2015 and 2019, respectively.

He is currently a Postdoctoral Researcher at the Oxford Robotics Institute, University of Oxford with I. Havoutis. During his Ph.D, he works on trajectory optimization and warm-starting optimal control for high-dimensional systems and humanoid robots under the supervision of S. Vijayakumar. His research

interests include fast optimization-based methods for planning and control, loco-manipulation, and legged robots.



Josep Marti-Saumell received the B.Sc. degree in industrial engineering (majoring in mechanics) and the M.Sc. degree in automatic control and robotics from the Universitat Politècnica de Catalunya, Barcelona, Spain, in 2013 and 2018, respectively.

He is currently a Ph.D. candidate at the Institut de Robòtica i Informàtica Industrial, CSIC-UPC, Barcelona, Spain. In 2014, he co-founded BonaDrone, a company devoted to educational robotics focused on 3D printed and programmable quadcopters. He also was CTO of BonaDrone from 2014 to 2019. His current research interests include optimal control applied to mobile robotics, numerical optimization, and unmanned aerial manipulators.



Joan Solà received the M.Sc. degree in telecommunication and electronics from the Universitat Politècnica de Catalunya, Barcelona, Spain, and the Ph.D. degree in robotics from the University of Toulouse, Toulouse, France, in 2007.

He is currently a Ramón y Cajal Researcher with the Institut de Robòtica i Informàtica Industrial, CSIC-UPC, Barcelona, Spain. He has also worked in the industry in the renewable energies sector, and was involved in the construction of a manned submarine for depths up to 1200 m. He has contributed to monocular SLAM, especially in the undelayed initialization of landmarks, and is interested in state estimation for robots with particularly large dynamics and degrees of freedom, such as humanoids and aerial manipulators. His current projects turn around whole-body estimation and control, including multisensor fusion, localization and mapping, machine learning, and model predictive control.



Nicolas Mansard received the M.Sc. degree in computer science from the University of Grenoble, Grenoble, France, in 2003 and the Ph.D. degree in robotics from the University of Rennes, Rennes, France, in 2006.

He has been a CNRS Researcher since 2009. He was then Postdoctoral Researcher at Stanford University, Stanford, CA, USA with O. Khatib in 2007 and in JRL-Japan with A. Kheddar in 2008. He was Invited Researcher at the University of Washington with E. Todorov in 2014. He received the CNRS Bronze Medal in 2015 (one medal is award in France in automatic/robotic/signal-processing every year). His main research interests include the motion generation, planning and control of complex robots, with a special regard in humanoid robotics. His expertise covers sensor-based (vision and force) control, numerical mathematics for control, bipedal locomotion and locomotion planning. He published more than 70 papers in international journals and conferences and supervised 10 Ph.D. thesis.

Dr. Mansard is currently an Associate Editor of the IEEE TRANSACTIONS ON ROBOTICS.



Sethu Vijayakumar received the Ph.D. degree in computer science and engineering from the Tokyo Institute of Technology, Tokyo, Japan, in 1998.

He is Professor of Robotics and a Director with the Institute of Perception, Action, and Behavior, School of Informatics, University of Edinburgh, U.K., where he holds the Royal Academy of Engineering Microsoft Research Chair in Learning Robotics. He also has additional appointments as an Adjunct Faculty with the University of Southern California, Los Angeles, CA, USA and a Visiting Research Scientist with the RIKEN Brain Science Institute, Tokyo. His research interests include statistical machine learning, robotics, planning and optimization in autonomous systems to human motor control, and optimality. Dr. Vijayakumar is a Fellow of the Royal Society of Edinburgh.